Annals of Biomedical Engineering, Vol. 51, No. 4, April 2023 (© 2023) pp. 702–714
https://doi.org/10.1007/s10439-023-03135-y

Original Article

Ex Vivo Uniaxial Tensile Properties of Rat Uterosacral Ligaments

KANDACE DONALDSON and RAFFAELLA DE VITA

STRETCH Lab, Department of Biomedical Engineering and Mechanics, Virginia Tech, 330A Kelly Hall, 325 Stanger Street, Blacksburg, VA 24061, USA

(*Received 2 November 2022; accepted 2 January 2023; published online 18 January 2023*)

Associate Editor Stefan M. Duma oversaw the review of this article.

Abstract—This manuscript presents new experimental methods for testing the *ex vivo* tensile properties of the uterosacral ligaments (USLs) in rats. The USL specimens ($n = 21$) were carefully dissected to preserve their anatomical attachments, and they were loaded along their main *in vivo* loading direction (MD) using a custom-built uniaxial tensile testing device. During loading, strain maps in both the MD and the perpendicular direction (PD) were collected using the digital image correlation technique. The mean (± S.E.M.) maximum load and displacement at the maximum load were 0.98 ± 0.30 N and 17.53 ± 3.87 mm, respectively. The USLs were found to be highly heterogeneous structures, with some specimens experiencing strains in the MD that were lower than 5% and others reaching strains that were up to 60% in the intermediate region. At 0.5 kPa stress, a value reached by all the specimens, the mean strain in the MD was $9.15 \pm 1.30\%$ while at 5 kPa stress, a value achieved only by 9 out of the 21 specimens, the mean strain increased to $23.87 \pm 3.64\%$. Under uniaxial loading, the specimens also elongated in the PD, with strains that were one order of magnitude lower than the strains in the MD; at the 0.5 kPa stress, the mean strain in the PD was recorded to be $0.69 \pm 0.66\%$ and, at the 5 kPa stress, the strain in the PD was $6.99 \pm 2.87\%$. The directions of maximum principal strains remained almost unchanged with the increase in stress, indicating that little microstructural re-organization occurred due to uniaxial loading. This study serves as a springboard for future investigations on the supportive function of the USLs in the rat model by offering guidelines on testing methods that capture their complex mechanical behavior.

Keywords—Uterosacral ligaments, Uniaxial testing, Digital image correlation, Tensile properties, Deformations, Heterogeneity.

INTRODUCTION

The uterosacral ligaments (USLs) are important anatomical structures that support the uterus and upper vagina through their connections to the sacral spine. These fan-shaped, membrane-like structures are comprised of connective tissue, adipose tissue, smooth muscle, blood vessels, nerves, and lymphatics. The components of the USLs are distributed differently along the length of the ligaments: the distal (closer to the cervix) region has a dense network of smooth muscle fibers and nerves whereas the proximal (closer to the sacrum) region primarily has loosely-organized connective tissues. The intermediate region, between the proximal and distal regions, has a gradient of smooth muscle and connective tissue components.[5,10,33] These microstructural differences likely impact the supportive function of the USLs.

Due to their critical role in supporting the reproductive organs, the USLs are often used in reconstructive surgeries for pelvic organ prolapse. Pelvic organ prolapse is a disorder characterized by the descent of the pelvic organs from their normal anatomical positions. In severe cases, this disorder is surgically treated to restore support to the prolapsed organs. These surgeries, however, continue to have very low success rates.[2,12,25] For example, a recent study reported that 56% of women who underwent USL suspension for uterovaginal prolapse experienced a recurrence while, in comparison, 29% of women who received vaginal mesh hysteropexy had recurrent prolapse.[2] Similarly, vaginal hysterectomy with USL suspension resulted in a higher rate of prolapse recurrence compared to supracervical hysterectomy with mesh sacrocervicopexy.[12] These findings were further confirmed in another clinical trial where vaginal hys-

Address correspondence to Raffaella De Vita, STRETCH Lab, Department of Biomedical Engineering and Mechanics, Virginia Tech, 330A Kelly Hall, 325 Stanger Street, Blacksburg, VA 24061, USA. Electronic mail: devita@vt.edu

terectomy with USL suspension was compared to sacrospinous hysteropexy with graft.[25] Given the low success rate of prolapse surgeries that rely on USLs and the controversial use of surgical grafts,[13] there is a clear need to explore new surgical methods that use native tissues such as USLs and develop alternative surgical materials.

The supportive function of the USLs is often evaluated *via* mechanical testing. Several studies have characterized elastic and viscoelastic properties of USL tissues in humans, non-human primates, and swine, as presented in detail in our recently published review article.[10] While some investigators have conducted biaxial tests of the USLs in efforts to more relevantly investigate the mechanical behavior of these tissues,[1,7,11,26] uniaxial tests are often preferred as they can be conducted using relatively small tissue specimens. A summary of published studies where the USLs, with and without other neighboring tissues, *ex vivo* or *in vivo*, were loaded along one single axis is presented in Fig. 1. Human tissues have been tested to determine the effects of parity,[21,27] pelvic organ prolapse, aging, and menopause on the mechanics of the USLs, reporting significant differences in the uniaxial elastic properties of tissues affected by pelvic organ prolapse.[27] The elastic and viscoelastic behavior of the apical vaginal supports have been tested *in vivo* with no reported statistical difference between the tissues of patients with and without prolapse due to small sample size.[18,30] Human and swine USLs have been shown to be stronger and less compliant than other similar supportive tissues, including the broad,[28] round,[28] and cardinal[31] ligaments. While testing human tissue is ideal, the tissues often used in mechanical studies skew towards parous, diseased, and elderly because they are obtained either through biopsy during pelvic surgery or posthumously.[10] Non-human primates are considered the gold standard of animal models, and the effects of hormone replacement therapies on the mechanics of ovariectomized macaques have been

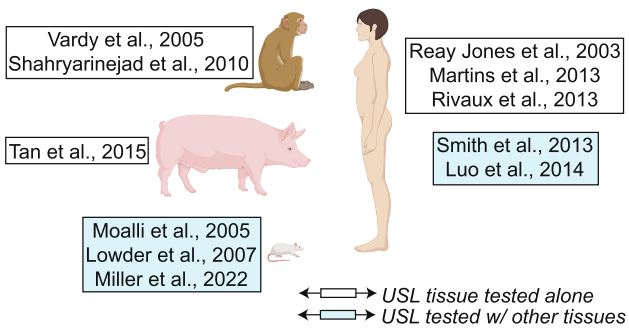

FIGURE 1. Summary of experimental studies where the USLs were subjected to uniaxial loading (in isolation or with other tissues, *ex vivo* or *in vivo*). These studies were conducted in rats, swine, monkeys, and human subjects.

investigated,[29,32] but studying their tissues introduces numerous ethical concerns and significant costs. Large animal models, such as swine, are promising as swine USLs appear to be mechanically and histologically similar to those of humans.[1] However, large animal species require specialized veterinary care, housing, and surgical facilities, increasing research costs.

Establishing the rat as a model for testing the mechanics of the USLs would allow investigators to control conditions such as parity, pregnancy, menopause, age, and hormone therapy. Rat USLs have been shown to be histologically similar to human USLs,[14] and a few studies have introduced rodent animal models for investigating the mechanics of pelvic organ support. These studies have involved the testing of the USLs with all of their surrounding organs and tissues still attached.[17,22,23] Moalli *et al.*[23] and Lowder *et al.*[17] tested the entire rat pelvis, fixed by the lumbar spine and adjacent bony pelvis, while the vagina was pulled caudally to failure. These authors reported stiffness parameters and failure loads of the combined pelvic organ supports for nulliparious, pregnant, and parous rats. Very recently, new methods have been proposed for testing the rat USLs by fastening umbilical tape around them *in situ* and pulling the tape upward with the rat in a supine position.[22] However, no experimental studies have been conducted on the mechanics of the rat USLs in isolation from the other pelvic organs and tissues, likely due to difficulties in distinguishing the USLs from surrounding tissues and in excising large enough portions of the USLs to mechanically test.

Previous studies have measured the deformations of the USLs using either grip-to-grip displacement or non-contact optical methods. It has been documented that deformation measurements that are based on grip-to-grip displacement can greatly overestimate the specimen's strain.[4,20,34] In accordance with Saint-Venant's principle, stating that the effects of the clamps can be ignored at points reasonably far away from them, some investigators have tracked the displacement of four points in the middle of the tested USL specimens using video cameras to compute their deformations.[7,31] However, these methods do not account for differences in strains that may result from the inherent material heterogeneity of the tissues. Over the past few years, the digital image correlation (DIC) method has been used to optically track speckle patterns created on the surface of the USLs, allowing for highly accurate strain measurements.[1,11,26] As previously mentioned, the USLs have a highly different microstructure in the proximal, intermediate, and distal regions, but how deformations may vary in these regions remains to be investigated. The DIC method can thus be used to obtain detailed information about

the strains in each of these regions if the entire USLs, rather than some specific anatomical regions, are mechanically tested.

In this manuscript, we present new experimental methods for testing the *ex vivo* uniaxial tensile properties of the USLs isolated from rats with their attachments to the cervix/vagina and the spine. Given the highly heterogeneous structure of the USLs, we use the DIC method to perform full-field strain measurements during uniaxial tensile testing. Together with load-displacement behavior, we determine the deformations of the rat USLs in the main *in vivo* loading direction (MD) and in the perpendicular direction (PD) as well as anatomical differences across the proximal, intermediate, and distal regions. New experimental techniques, analysis, and data that characterize the mechanical function of the USLs as those proposed here could guide the development of scientific-based surgical guidelines and biomaterials for USL suspension procedures.

METHODS

Specimen Preparation

This study was conducted with approval from the Institutional Animal Care and Use Committee (IACUC) at Virginia Tech. A total of 21 virgin Sprague-Dawley rats, aged 13–14 weeks, were sourced from a separate research group that had been conducting memory-related behavioral studies. All rats used in this study received the same treatment and living conditions in accordance with the ethical guidelines of the National Institutes of Health. Prior to mechanical testing, the rats were euthanized *via* decapitation and stored at −20 °C for 1–2 months. The rats were thawed at 4 °C for 2–4 days, though due to the rats' bulk, they remained partially frozen until they were further thawed at room temperature (20–25 °C) for 2–3 h on testing days.

The USLs were excised from the rats using a dissection technique that preserved the proximal and distal attachments of the ligaments. Specifically, each rat was laid on a dissection mat in supine position. A midline incision was made using sharp surgical scissors starting at the caudal aspect of the rib cage and extending beyond the pelvis, stopping short of the vaginal introitus. The abdominal walls were retracted, the intestines were displaced cranially to better visualize the remaining surrounding organs within the abdominal and pelvic cavities. Then, the secondary connective tissue and fascia between the vagina and the pubic symphysis (part of the Level II support as defined by DeLancey[8]) were severed with small surgical scissors, separating the vagina from the pelvis, and the pubic symphysis was severed (Figs. 2a, 2b). The vaginal introitus was isolated from the connected perineal tissues (Fig. 2b). The pubic-ischial junction was cut to allow removal of the pubic arch (Fig. 2c. The ovaries, oviducts, and uterine horns were exposed and separated from their surrounding connective tissues so that they could be moved freely (Fig. 2c). However, the more caudal connective tissues near the cervix were avoided to minimize risk of damaging the USLs. Since the USLs wrap around the rectum to attach at the sacral spine, the rectum was carefully removed from the uterine and vaginal supports to excise the entire USLs without damage (Fig. 2d). To accomplish this, small surgical scissors were used to sever the rectum from all of its surrounding connective tissue, including the tissue between the rectum and the vagina/cervix, in small flush cuts against the rectal wall until the rectum was detached on all sides and could be pulled through the pelvic cavity with no resistance (Fig. 2e). Throughout this process, the distal portions of the USLs were identifiable by moving the uterus to an anteverted position (Figs. 2f, 2g).

In order to preserve and excise the vagina, cervix, uterus, USLs, and sacral/lumbar spine as one intact complex, any attached musculature, connective tissue, and vasculature were severed as close to the body wall as possible, allowing elevation of the complex from the caudal and lateral regions of the pelvis (Figs. 2e–2g). The pelvic girdle was separated from the pelvic spine by cutting through the articular surfaces of the ilia. The uterus and vagina were shifted to the opposite side of cutting at all times so that, together with their connective tissues, they could be visualized and avoided. Then, surgical bone cutting forceps were used to sever the lumbar spinal column, cranially to the isolated reproductive tract and connective tissues and caudally to the sacrococcygeal joint. The connective tissue between the dorsal aspect of the spine and the dorsal peritoneum was cut, detaching the reproductive tract/spinal segment complex (Fig. 2h). The complex shown in Fig. 3a was removed from the rat body and spread on the dissection board. The USLs were inspected, and if one of the ligaments sustained damage from the dissection, then the other one was selected for testing. Otherwise, selection of right vs. left USL was arbitrary. The extra USL was severed, and excess tissue was removed to yield the final specimen, consisting of the sacrum, the USL, the cervix, the apical vagina, and a small amount of miscellaneous muscle and connective tissue that could not be removed without risking the integrity of the USL (Fig. 3b). Since the exact connection points of the USLs at the sacrum are indirect and arbitrary, inclusion of some excess tissue along the spine was inevitable. The specimens were

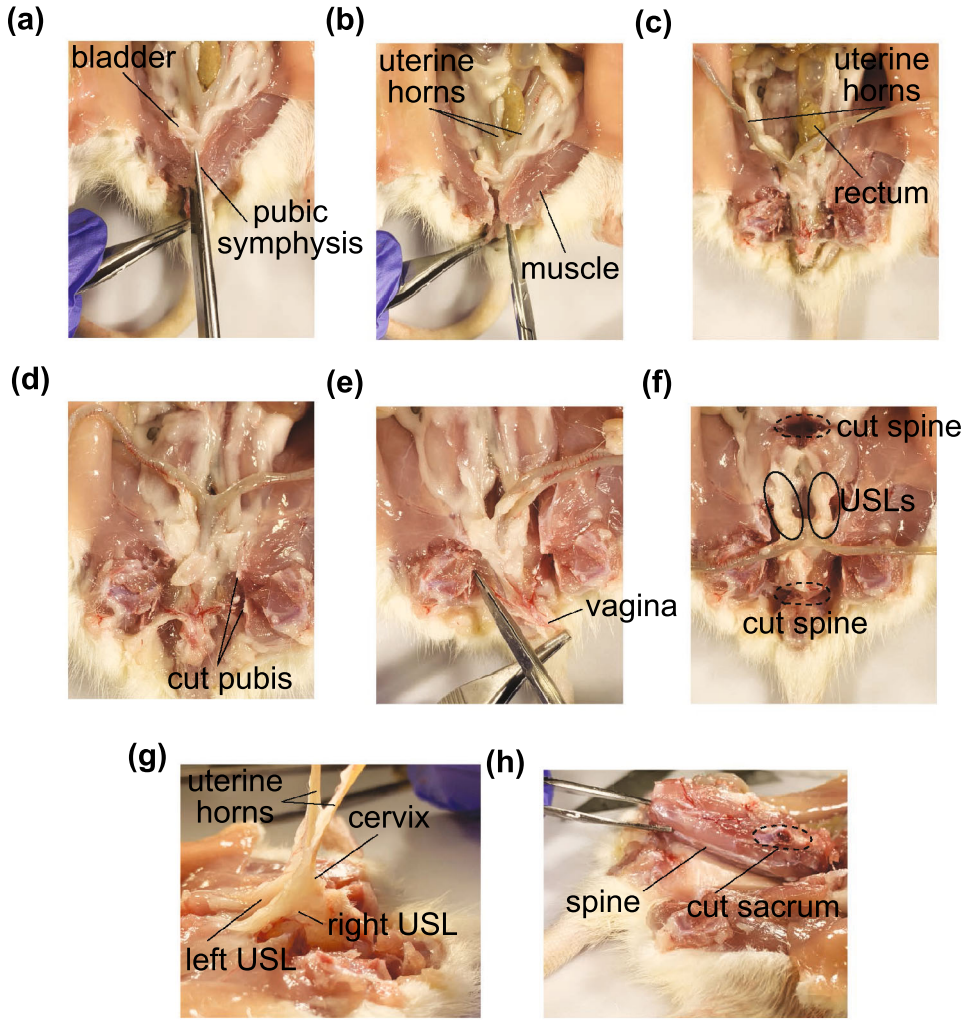

FIGURE 2. Pictures of the rat pelvis (ventral view) showing some major steps during the dissection of the USL specimen. (a) Severing of the pubic symphysis following the opening of the abdominal walls. (b) Isolating of the vaginal introitus. (c) Exposing the ventral vagina as well as the uterine horns after cutting pubic bones. (d) Showing the same features as (c) after removal of the rectum. (e) Severing of the vagina, cervix, uterus, USLs, and spine complex from the pelvic sidewall. (f) Vagina, cervix, uterus, USLs, and spine complex severed from the ventral and lateral pelvis, cuts through the caudal and lumbar vertebrae, with the uterus in an anteverted position, exposing the distal USLs to view. (g) Side view of the vagina, cervix, uterus, USLs, and spine complex with the anteverted uterus extended ventrally, exposing the distal USLs to view. (h) Excision of the vagina, cervix, uterus, USLs, and spine complex following separation from the pelvic girdle, during the severing of connective tissue from the dorsal aspect of the spine.

kept hydrated during dissection by intermittent application of PBS. The thickness of each specimen was measured using a CCD laser displacement sensor (LK-G82, Keyence, Inc., Japan) at six random points of the USL, two in each anatomical (proximal, intermediate, or distal) region (Fig. 3b) (Table 1).

Mechanical Testing

Prior to testing, the USL specimens were speckled with matte black quick-drying spray paint applied through a mesh screen, held under gentle airflow to dry, and then gently hydrated with PBS. The specimens were then mounted at their proximal and distal ends using specially-designed 3D printed clamps. At the proximal/spinal end, the preserved spinal segments were clamped in a 3D printed vise-style L-shaped clamp with ridged surfaces to prevent the specimens from slipping. At the distal/cervical end, the specimens were mounted on a 3D printed block holding three L-shaped needles, spaced 3.5 mm, which were used to puncture the specimens at the cervical/vaginal attachments. Once clamped, the specimens were loaded into a custom-built tensile testing apparatus consisting of two linear actuators with 25 mm stroke length and 0.048 μm micro-step size resolution (T-NA08A25,

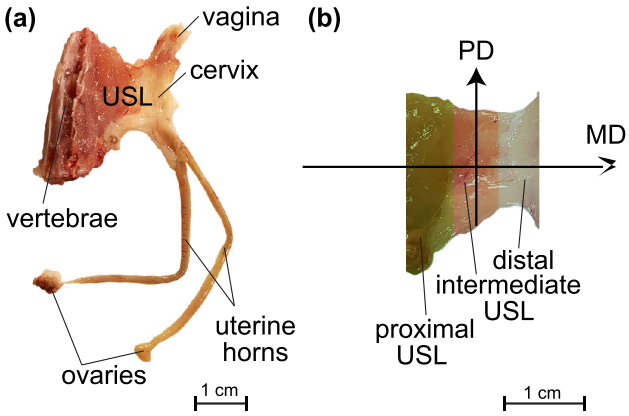

FIGURE 3. (a) USL with its attachments to the spine and cervix/vagina/uterine horns. (b) USL specimen used for uniaxial testing showing the proximal, intermediate, and distal regions.

TABLE 1. Mean (± S.D.) thicknesses and widths of the USL specimens in their three anatomical regions ($n = 21$)

	Proximal	Intermediate	Distal
Thickness (mm)	4.23 ± 1.21	2.97 ± 0.51	2.48 ± 0.51
Width (mm)	16.71 ± 1.54	13.30 ± 1.55	12.24 ± 1.16

The mean clamp-to-clamp length for the specimens was 18.20 ± 1.21 mm.

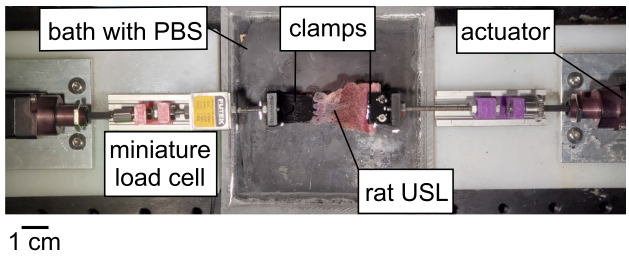

FIGURE 4. Picture of the rat USL with attachments to the cervix/vagina and spine mounted on the custom-made uniaxial testing system.

Zaber Technologies, Inc., Vancouver, BC, Canada), an 8.9 N-capacity and 0.1% accuracy load cell (FSH00092, Futek Advanced Sensor Technology, Inc., Irvine, CA), and a tissue bath filled with PBS (Fig. 4). Then the specimens were pre-loaded up to 5 mN at a rate of 10 μm/s to ensure that prior to collecting load data and calculating strain, all specimens were relatively flat and not bunched up and folded. Since parts of the USLs were fragile, especially the top speckled layer, the specimens were not preconditioned, as the procedure would likely have damaged the tissues. Following this step, the specimens were loaded to ultimate failure at 10 μm/s or until the actuator stroke limit was reached while images were collected at 1 Hz. All testing protocols were programmed in LabVIEW (NI, Austin, TX).

DIC Imaging and Strain Analysis

During the mechanical tests, high-resolution (2448 × 2048 pixels) images were taken at 1 Hz using two CMOS cameras (Basler ace acA2440-75 μm, Basler, Inc., Exton, PA) positioned at different angles. The cameras were focused on the speckled specimens and calibrated using a standard calibration grid with 3 mm spacing. The collected images were processed using a DIC system (Vic-3D, version 9, Correlated Solutions Inc., Irmo, SC). Axial Lagrangian strains in the main *in vivo* loading direction (MD) and the perpendicular direction (PD) were calculated over roughly 0.5 cm^2 selected areas of interest (AOI) within each of the three anatomical (proximal, intermediate, and distal) regions of the USLs, along their longitudinal mid line. The average values were taken for each AOI at each second until the system stopped being able to track the speckles. Mean axial Lagrangian strains in the MD and in the PD will be referred to as "strain in the MD" and "strain in the PD," respectively. The reference configuration, associated with zero strain, was selected to be that at the preload of 5 mN. Nominal (normal) stresses in the MD, or "stress in the MD," for each anatomical region were calculated by normalizing the force data obtained from the load cell by the cross-sectional areas of the USLs. These cross-sectional areas were calculated in each of the three anatomical regions by multiplying the thickness and width of such regions. The width in the three anatomical regions and the clamp-to-clamp length of the USLs were measured in ImageJ (NIH, Bethesda, MD) from images of the specimens collected in the reference configuration (Table 1) .

Maximum/minimum principal strains and the corresponding directions of principal strains were also computed using the DIC system in the intermediate regions of the USLs at equivalent stress values in the MD. For each specimen, the directions of principal strains were calculated locally within the AOI of the intermediate region. The MD was defined to be at 0° angle while the PD was assumed to be either at 90° and − 90° angles.

The strains in the MD at equivalent stresses for the tested USLs were statistically compared between the three anatomical regions using one-way ANOVAs with a confidence interval of 95%. All averaged data in this manuscript are reported with the standard error of the mean (i.e., mean ± S.E.M.) unless otherwise specified.

RESULTS

Uniaxial load-displacement data in the MD for the tested rat USLs are reported in Fig. 5. The presence of several peaks in the load as the displacement increased

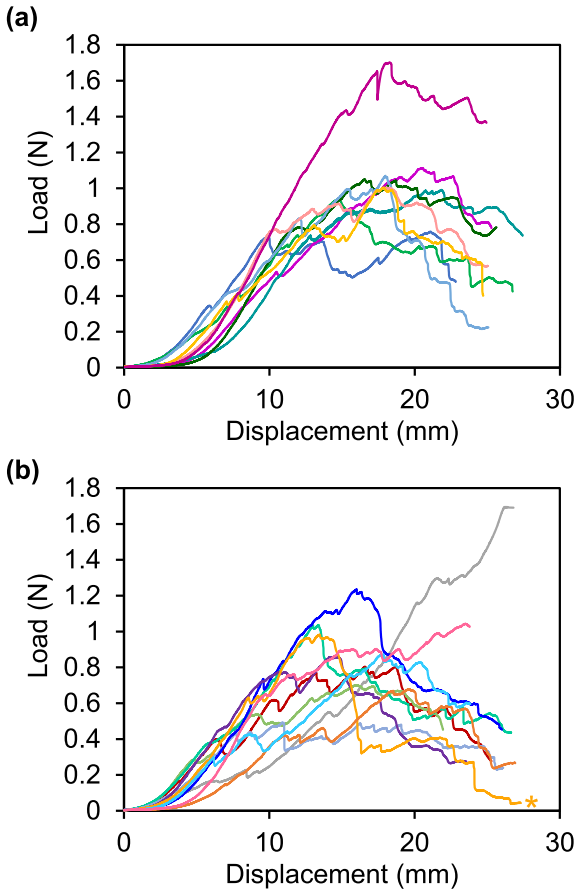

FIGURE 5. Load-displacement data collected from $n = 21$ rat USLs up to failure. Data are presented in two sub-figures, (a) and (b), for clarity. Curves in different colors represent different specimens. The yellow asterisk identifies data relative to a selected representative specimen.

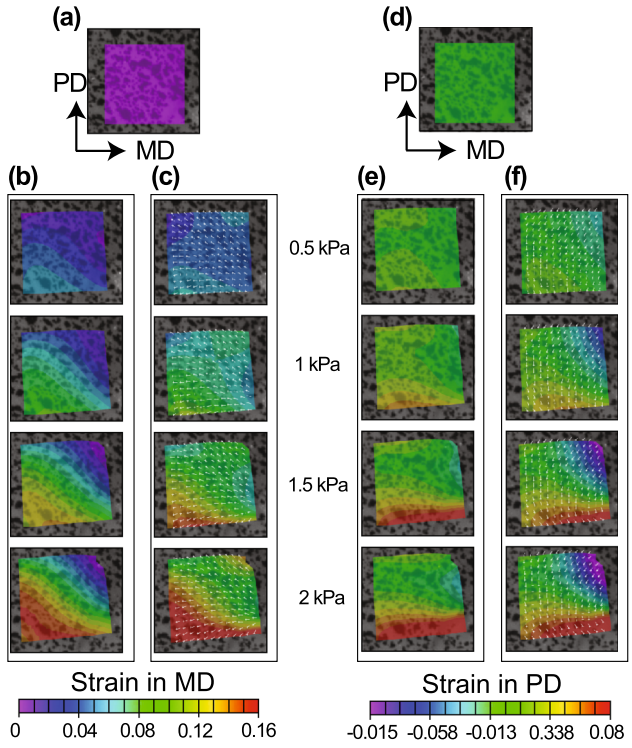

FIGURE 6. DIC strain maps in the intermediate region of a selected representative rat USL (specimen curves identified in other figures with yellow asterisks) in the MD and PD during uniaxial testing at increasing stress values of 0.5, 1, 1.5, and 2 kPa in the MD. (a) Strain map in the MD at preload. (b) Strain maps in the MD at different stress levels. (c) Map of maximum principal strains and corresponding directions of maximum principal strains. (d) Strain map in the PD at preload. (e) Strain maps in the PD at different stress levels in the MD. (f) Map of minimum principal strains and corresponding directions of minimum principal strains.

clearly demonstrates that the failure of the USLs occurred gradually, with bundles of fibers breaking at various load levels. Despite the variability observed across all the specimens, the load-displacement data were characterized by an initial toe region, an almost linear region, and then a nonlinear failure region as one would expect for soft tissues. The maximum loads experienced by each specimen ranged from 0.49 to 1.70 N with the average maximum load being 0.98 ± 0.07 N. The displacements at which the maximum loads occurred ranged from 10.92 to 26.18 mm with the average being 17.53 ± 3.87 mm.

Strain data in the MD and PD were successfully collected for all tested specimens ($n = 21$) but, due to the gradual failure of the USL specimens, these data were not collected for the entire duration of the tests. Examples of strain maps that were obtained for one USL specimen in the intermediate region using the DIC method are reported in Fig. 6. From Figs. 6a, 6b and 6d, 6e, one can observe the specimen in the reference configuration and at different stress values along the MD and PD, respectively. Maps of maximum and minimum principal strains as well as their corresponding directions are reported in Figs. 6c and f, respectively. As expected, the differences between the strains and principal strains (Figs. 6b vs. 6c and 6e vs. 6f) were not noticeable so only strains in the MD and PD are reported hereafter.

Stress-strain data in the MD for all the tested specimens in the intermediate region are reported in Fig. 7. For some specimens strains lower than 5% were measured (see Fig. 7a, red curve), but for other specimens strains up to 60% were recorded (Fig. 7b, gray curve) before the tissues started to break. The stresses experienced by the specimens at the point of failure of the speckled USL layers ranged from 0.71 to 7.91 kPa with an average value of 4.13 ± 0.46 kPa.

Mean stress data in the MD vs. strain data in the MD computed from $n = 18$ USLs in the distal region, $n = 21$ USLs in the intermediate region, and $n = 17$ USLs in the proximal region are reported in Fig. 8a. Due to deterioration and variability of the speckle

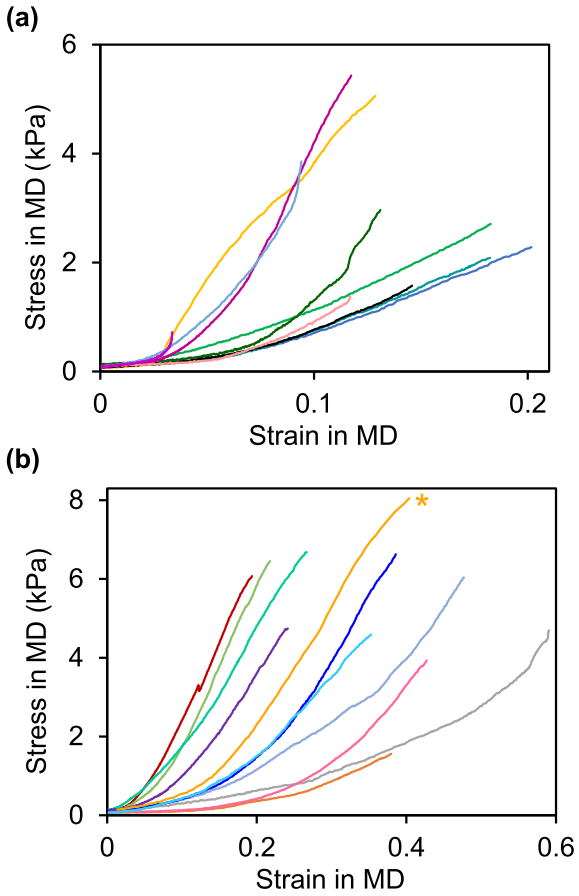

FIGURE 7. Stress-strain data in the MD for the intermediate regions of all tested USL specimens ($n = 21$). Data are presented in two sub-figures, (a) and (b), for clarity. Curves in different colors represent different specimens. The yellow asterisk identifies data relative to a selected representative specimen.

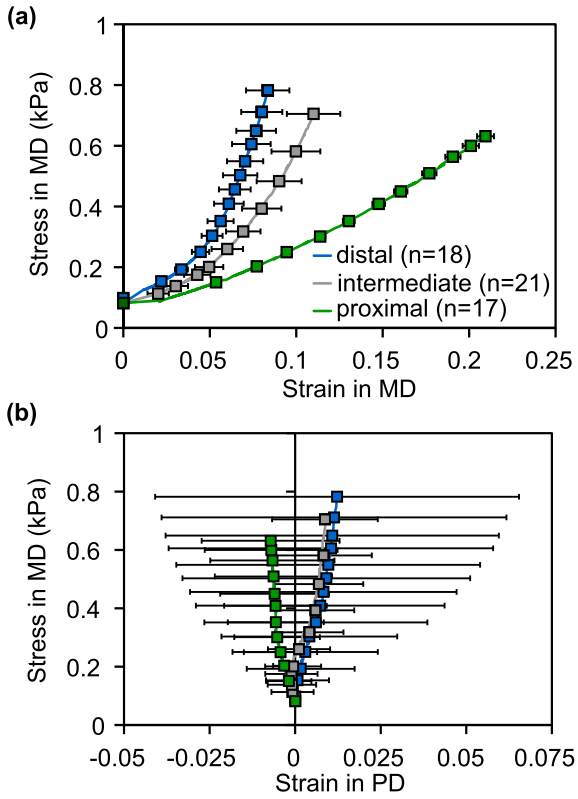

FIGURE 8. Mean (± S.E.M) strain data in the (a) MD and (b) PD computed at three anatomical regions of the USL vs. stress data in the MD.

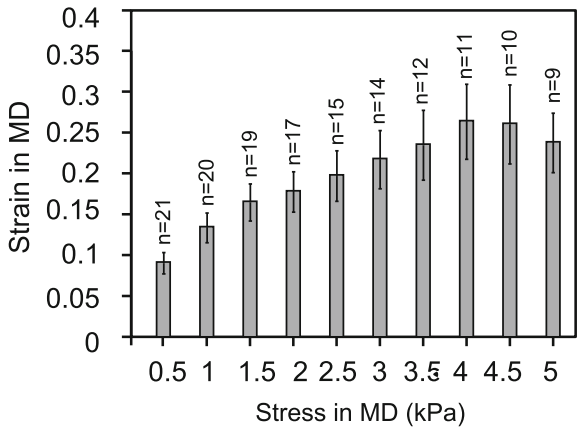

FIGURE 9. Mean (±S.E.M.) strain data in the MD for the intermedial region at various values of the stress. Since specimens reached different stress levels, the number of specimens in each group is different as reported in the chart.

patterns, strain data could not be calculated in every region for all $n = 21$ specimens. Because the reported data are averaged, they were computed only up to the highest strains achieved in each region by all the USLs. Though not statistically significant with a 95% confidence interval, in the MD, the USLs tended to be stiffest in their distal regions and most compliant in their proximal regions. Strains in the MD were tracked in each region of every specimen at stresses of 0.6 kPa. At 0.6 kPa stress, strain in the distal region almost reached 7.4%, strain in the intermediate region reached 10%, and strain in the proximal region was greater than 20% (Fig. 8a). As the specimens were uniaxially loaded in the MD, they strained both along the MD and PD. Figure 8b shows stress data in the MD vs. strain data in the PD. On average, the strain in the MD was one order of magnitude higher than the strain in the PD in the intermediate region. While strains in the PD in the distal and intermediate regions mostly averaged to positive numbers, the average strain in the PD in the proximal region was negative at all measured stresses. However, much more variability was observed for the strains in the PD than for the strains in the MD, relative to the magnitude of the strains; both negative and positive values of strain in the PD were observed in different specimens. Average values of stress and strain in the MD for the intermediate region are reported at higher values of stress in Fig. 9, noting the

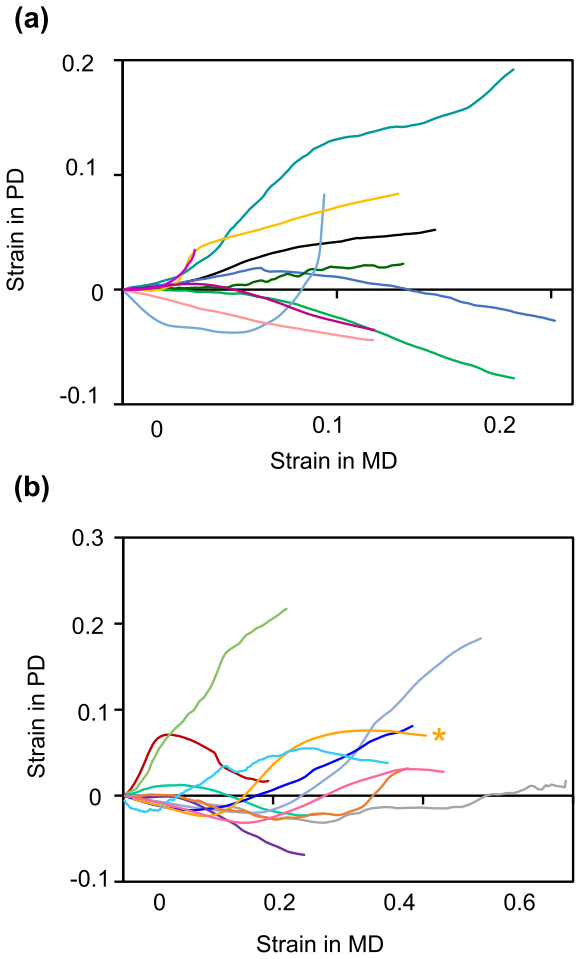

FIGURE 10. Strain data in the MD and PD in the intermediate region ($n = 21$). Data are presented in two sub-figures, (a) and (b), for clarity. The yellow asterisk identifies data relative to a selected representative specimen.

number of specimens for which strain could be tracked at each stress value. One may find approximate secant moduli by dividing the stress values by their corresponding strain values reported in this figure.

Strain data in the PD vs. strain data in the MD for the intermediate regions of the USLs are reported in Fig. 10. This figure shows that, as the strain in the MD increased in the intermediate region, the strain in the PD was sometimes negative (as one would expect), was at other times positive, and in a few cases was almost zero. However, average values of the strain in the PD were consistently positive at the corresponding values of strain in the MD up to 25% strain in the MD (Fig. 11). These average values of strain in the PD consistently increased with increasing strain in the MD.

The angles of maximum principal strains in the intermediate region aligned mostly around the MD, the direction of loading defined as 0°, with the vast majority of angles falling between −45° and 45° for

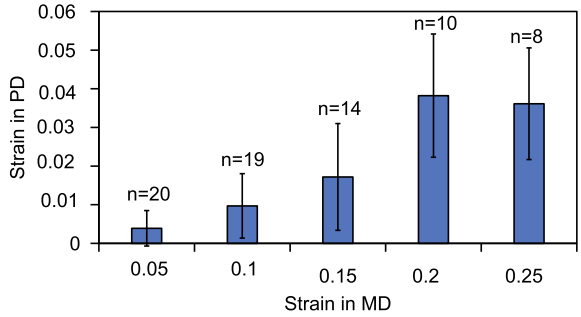

FIGURE 11. Mean (±S.E.M.) strain data in the MD vs. strain data in the PD in the intermediate region. Since specimens reached different strain levels, the number of specimens in each group is different as reported in the plot.

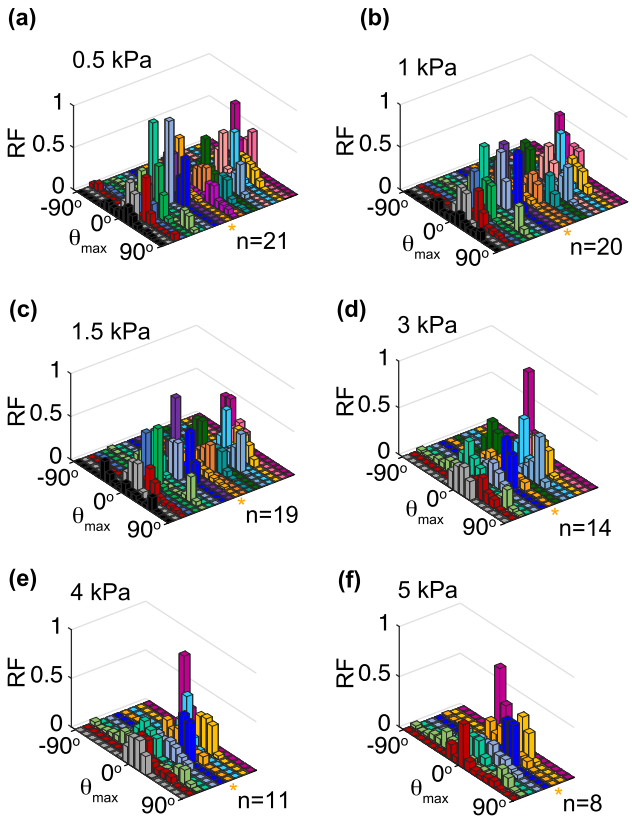

FIGURE 12. (a–f) Relative frequency (RF) distributions of directions (θ_{max}) of maximum principal strains at stress values of 0.5, 1, 1.5, 3, 4, and 5 kPa for n =21, 20, 19, 14, 11, and 8 specimens, respectively. Data in different colors are from different specimens and data in the same colors are from the same specimens. Note that the number of distributions/specimens in each subfigure changes since the tested specimens reached different stress values. The MD is at 0° while the PD is at ±90°. The yellow asterisk identifies data relative to a selected representative specimen.

each specimen (Fig. 12). This remained consistent at each stress value of 0.5, 1, 1.5, 3, 4, and 5 kPa in the MD. The number of principal direction distributions that could be computed decreased at increasing stress values as not all specimens reached the same level of

stress (Fig. 12). At 0.5 kPa stress in the MD, almost 30% of the maximum principal strain angles in the intermediate region for all USLs ($n = 21$) were aligned between $-5°$ and $5°$, and the remaining 70% of angles were more than $5°$ away from the MD but still close to such direction. Almost 10% of angles were between $\sim 45°$ and $\sim -45°$, or halfway in between the MD and the PD.

DISCUSSION

This study presents the experimental methodology for measuring the tensile properties of the most important apical support structures of the vagina, the USLs, using the rat as an animal model. By adopting a dissection technique that isolated the entire USLs and using a custom-made tensile testing device, we measured load-displacement data along the main *in vivo* loading direction of these ligaments. We also measured the strain in both the main *in vivo* loading direction (MD) and the transverse direction (PD) using the DIC method. To the authors' knowledge, there are no other experimental studies that attempt to test the mechanical properties of the rat USLs. This experimental work is especially important since the rats are convenient for biomedical research, and they can be genetically modified to induce prolapse and other pelvic floor disorders. Moreover, a recent comparative histological study suggested several similarities between rat and human USLs making the rat an ideal choice for future biomedical studies.[14]

While load-displacement data of the entire vagina with the attached USLs have been collected by Moalli *et al.*[23] there are currently no other mechanical studies in which the rat USLs have been tested along their physiological loading direction. Very recently, experimental methods to test the integrity of rat USLs *in situ* after USL suspension have been developed but, again, the USLs were pulled with the attached organs.[22] Ideally one should be able to fully isolate the USLs from any other tissues, but this is very challenging given the small size of the USLs in the rats. The dissection procedure employed in this study was involved and required great care to avoid placing cuts near the USLs or their connections. Without retaining their connections, the USLs become almost impossible to distinguish from surrounding tissues and hard to excise. When the tension provided by the sacral and cervical attachments are missing, the rat USLs lose their shapes and form amorphous blobs. For this reason, our dissection technique was devised to excise the USLs with their intact attachments. The proposed technique is time-consuming and complicated, but it gave us confidence that entire USLs, with the three anatomical regions, were correctly identified and removed. Although our goal was to isolate the USLs from their attachments, we retained both attachments at the vagina/cervix and the spine to facilitate clamping within our custom-made tensile testing device and measured the tensile properties of the USLs. Moreover, had we separated the USLs away from the spine, the location of separation would have been arbitrary and, therefore, we decided to keep the spinal connections intact to test the entire USLs.

The load-displacement curves reported in Fig. 5 are characterized by a toe region followed by a linear region, as typically observed for soft biological tissues. The curves exhibited an extended nonlinear region that had local minima and maxima indicating a gradual failure of the USLs before complete rupture. Due to the USLs' many components (collagen, elastin, muscle, fat, and nerve fibers), the failure behavior was quite complex, being determined by these components and their relative organization. During testing, breakage of collagen and smooth muscle bundles could be visually detected at the start of the gradual failure process. The load appeared to be carried out by collagen bundles alone at the end of the test, often being stretched tens of μm before breaking. The highest load that any of the USLs in this study experienced was lower than 2 N. In comparison, the ultimate load at failure reported by Moalli *et al.*[23] ranged between 11.8 N and 15.3 N. This factor of 10 difference may be explained by the nature of the specimens. Moalli *et al.* kept the entire rat pelvis intact and pulled on the vagina, effectively testing the entire pelvic organ support system while we tested only the USLs excised from the rest of the pelvic support tissues. Tan *et al.*[31] uniaxially tested post-partum sow USLs and found their mean ultimate strength, or the maximum stress experienced by the specimens, to be 2.767 ± 0.444 MPa. This value was a factor of 100 higher than the ultimate strength of the rat USLs, 13.17 ± 8.94 kPa, indicating that the sow USLs are much stronger than the rat USLs. Although a comparative study is needed to understand how the USLs may adapt in different species to achieve their mechanical function, the large size of the pelvic organs in sows likely require USLs with superior strength.

To our knowledge, this is the first time that the nonhomogeneous strains of the USLs are reported, in both the MD and PD. Not surprisingly, these strains were found to be much higher in the MD than in the PD (Fig. 6). When averaged across the intermediate regions of the USLs, the strains in the MD were as high as 60% before the DIC system became unable to track the speckle patterns on the surface of the specimens (Fig. 7). For some specimens, speckle-tracking became unfeasible after the USLs sustained very little strain (less than 5%). As expected, the stresses in the

MD corresponding to the measured strains also varied, from 0.7 kPa to 8 kPa. Even when compared at the same stresses, some variation along the achieved strains was noted (Fig. 9). The variability in stress-strain curves of USLs isolated from different animals, as well as the variability in the physical dimensions of the specimens (Table 1), has been reported in previous studies on both animal and human USLs[10]. This inter-subject variability may contribute to the high recurrence rate in surgical repair of pelvic organ prolapse, and it needs to be considered when developing new surgical techniques and graft materials. For example, the characteristics of graft materials must be tailored to the subjects' specific USL properties so that they can better integrate with the host tissues.

Tracking the speckle pattern that we created on the surface of rat USLs for DIC-based strain measurement proved to be challenging, primarily due to the layered structure that characterizes these tissues. Once the specimens were under load, the top speckled layer exposed to the cameras was observed to stretch and break revealing regions of the specimens that were underneath the speckled surface. This prevented the measurement of strain for the whole duration of the tests for all tested specimens after about 0.7 kPa in the MD (Figs. 9 and 12). Additionally, we experienced the usual challenges associated with performing DIC-based strain analysis on soft tissues, including difficulty in creating a highly-contrasted speckle pattern on soft tissue surfaces, which are naturally irregular, and degradation of the speckle pattern caused by immersion (e.g., in saline solution). For these reasons, the proximal and distal regions of some USL specimens could not be tracked, resulting in strain data collected only for a subset of USL specimens in these regions (Fig. 8). These issues suggest the need of complementary optical measurement methods to capture the deformation of the USLs as they are being loaded uniaxially. Recently, optical coherence tomography has been shown to provide encouraging results for the measurement of through-thickness deformations of the USLs.[11]

The morphological properties of the USLs in women have been described as being different in the proximal, intermediate, and distal regions. In this study, we defined the three regions of the USLs as equal thirds, as is the case for the majority of USL anatomical studies.[3,5,6,14] This definition is arbitrary, and methods have been proposed to classify the regions based on macroscopic differences in thickness, attachments to surrounding structures, and tissue contents.[33] No such studies have been conducted for USLs in rats or other animals so it is unknown how animal USLs vary by region or how closely these variations resemble those of human USLs. The difference in composition of these ligaments may affect their mechanical properties as one would expect the proximal portion of the USLs, with higher collagen content and looser organization, to be more compliant than the densely packed smooth muscle of the distal region. We did not find significant differences in strains among the three regions, though for some stresses at which comparisons were made (i.e., 0.5, 1, and 2 kPa), strains in the three regions were significantly different with a 90% confidence interval. The regional strains seemed to differ more at increasing stresses (Fig. 8). However, at increasing stresses, the results were reported with decreasing number of specimens, detracting from statistical power for comparisons at higher stress values (Fig. 9).

Our strain measurements in both the MD and PD suggested that the USL specimens got longer in the direction of loading (i.e., the MD), but strains in the transverse direction (i.e., the PD) were less consistent. This can be clearly observed in Fig. 10, where some specimens maintained positive strain in the PD during testing while other specimens experienced both positive and negative strains in the PD over the course of the tests. When the data were averaged, strain in the PD was consistently positive, indicating a negative Poisson ratio for the rat USLs (Fig. 11). This is unlike many other conventional materials subjected to uniaxial loading where the strain is negative in the transverse direction as the strain in the axial direction increases and remains positive. Such mechanical behavior is not uncommon for fibrous materials and materials with a complex micro-structure as the constituents (e.g., fibers) may reorganize during loading. Indeed, recent research has shown positive transverse strains for the articular anterior cruciate ligament using the DIC method, likely reflecting individual fiber bundles expanding laterally when pulled in their *in vivo* loading direction.[20] Other studies of the Achilles tendon have reported positive transverse strains and attributed them to the tendons' concave shape.[19,24] The dissected rat USLs also presented a concave shape, as seen in Fig. 3. Specifically, the lateral edges of the ligaments curved inward, with the greatest curvature in the distal region and the least curvature in the proximal region. During uniaxial tensile testing, the most concave regions of the USLs (i.e., the distal and intermediate regions) expanded in the transverse direction while the regions with the outermost lateral edges (i.e., the proximal region) slightly shrunk. This is reflected in the average distal, intermediate, and proximal strain curves in the PD in Fig. 8, likely revealing that these strains result from both the structural and material properties of the USLs. If the observed trends hold true for human USLs, this could have functional implications for the USLs' supportive role in preg-

nancy. As the load of the uterus increases and the USLs elongate along the main *in vivo* direction, a concurrent lateral extension of the ligaments could lead to an increase in their cross-sectional area. Such increase would reduce the amount of stress experienced by the ligaments, potentially offsetting the increase in stress caused by the increase in load of the uterus over the course of pregnancy. Our strain measurements may have also been affected by the clamping techniques: while the proximal end of the USL specimen was secured *via* mechanical clamps the distal end was clamped through three needles, giving a bit more freedom to the tissue to expand in the PD in the intermediate and distal regions.

In addition to strains in the MD and PD, maximum and minimum principal strains were also calculated. However, since the maximum principal strains were very similar to the strains in the MD and the minimum principal strains were very similar to the strains in the PD, the principal strains were not reported. These similarities were to be expected; since the specimens were pulled along the MD, naturally they strained most in that direction. The directions of maximum principal strains, calculated across the AOI in the intermediate region, are reported in Fig. 12. One can observe that the directions of principal strains for each specimen changed very little over the course of the tests as the stress increased. The majority of the maximum principal strains aligned with the MD, defined as 0° in Fig. 12, and remained so at each reported value of stress in the MD. These results give us confidence that the direction of loading aligned with the material axes of the USLs; the majority of the collagen fibers were likely aligned in the MD. If the specimens had experienced significant shear strain or if the collagen fibers reoriented significantly at an angle away from the MD, the histogram distributions would vary at the different stresses, rather than showing the consistency that they do.

The USLs are one of the most commonly used native tissues for restoring mechanical support to the prolapsed pelvic organs by way of corrective surgeries, but these surgeries remain problematic. Mesh materials for prolapse repair are historically controversial, with transvaginal meshes recently being banned by the FDA for high rates of complications, including pain, discharge, mesh erosion, and mesh exposure through the vaginal wall in the most severe cases.[9,13,16] Surgical procedures and materials to correct prolapse can be improved by gaining a better knowledge of the properties of pelvic tissues. Our study not only presented new methods for testing the USLs in rats but also offered new mechanical data about these ligaments, suggesting new research directions. If human USLs are indeed functionally graded auxetic materials, then performing USL suspensions with biomaterials having similar properties may improve patient outcomes. Synthetic meshes with a microstructure that leads to auxetic behavior may significantly impact surgeries by reducing mesh-related complications.[15] More research must be done to investigate whether the findings in this study hold true for USLs in women and how such findings are altered in women suffering from pelvic organ prolapse.

Conclusions

This experimental study presents the first *ex vivo* mechanical characterization of the rat USLs, providing measurements of the highly inhomogeneous deformations experienced by these important pelvic structures under uniaxial tensile loading. The USLs were excised using a novel dissection method that preserved their cervical and sacral attachments so that the deformations in three different anatomical (proximal, intermediate, and distal) regions could be computed using the DIC technique. The USLs elongated not only in the main *in vivo* loading direction (MD), as expected since loading was applied in that direction, but also in the perpendicular direction (PD). These results may have important implications for pelvic organ prolapse surgeries that rely on the use of USLs (e.g., USL suspension) and for novel surgical materials that augment the support function of the USLs. By adopting the rat as an animal model to study the mechanical properties of the USLs, the potential alterations that are induced by factors such as pregnancy, parity, aging, and prolapse can be controlled and investigated. Future mechanical studies will have to establish whether and/or to which degree the findings on rat USLs can be translated to human USLs.

ACKNOWLEDGMENTS

Funding was provided by National Science Foundation Grant No. 1804432. The authors would like to thank the Jarome Lab at Virginia Tech for providing the rats used in this study and Dr. Bonni Beaupied for providing feedback on the description of the dissection protocol in this manuscript.

CONFLICT OF INTEREST

The authors declare that they have no conflict of interest.

REFERENCES

[1]Baah-Dwomoh, A., M. Alperin, M. Cook, and R. De Vita. Mechanical analysis of the uterosacral ligament: Swine vs human. *Ann. Biomed. Eng.* 46(12):2036–2047, 2018.

[2]Bowen, S. T., P. A. Moalli, S. D. Abramowitch, M. E. Lockhart, A. C. Weidner, C. A. Ferrando, C. W. Nager, H. E. Richter, C. R. Rardin, Y. M. Komesu, et al. Defining mechanisms of recurrence following apical prolapse repair based on imaging criteria. *Am. J. Obstet. Gynecol.* 225(5):506, 2021.

[3]Buller, J. L., J. R. Thompson, G. W. Cundiff, L. K. Sullivan, M. A. S. Ybarra, and A. E. Bent. Uterosacral ligament: Description of anatomic relationships to optimize surgical safety. *Obstet. Gynecol.* 97(6):873–879, 2001.

[4]Butler, D. L., E. S. Grood, F. R. Noyes, R. F. Zernicke, and K. Brackett. Effects of structure and strain measurement technique on the material properties of young human tendons and fascia. *J. Biomech.* 17(8):579–596, 1984.

[5]Campbell, R. M. The anatomy and histology of the sacrouterine ligaments. *Am. J. Obstet. Gynecol.* 59(1):1–12, 1950.

[6]Collins, S. A., S. A. Downie, T. R. Olson, and M. S. Mikhail. Nerve injury during uterosacral ligament fixation: a cadaver study. *Int. Urogynecol. J.* 20(5):505–508, 2009.

[7]Danso, E. K., J. D. Schuster, I. Johnson, E. W. Harville, L. R. Buckner, L. Desrosiers, L. R. Knoepp, and K. S. Miller. Comparison of biaxial biomechanical properties of postmenopausal human prolapsed and non-prolapsed uterosacral ligament. *Sci. Rep.* 10(1):1–14, 2020.

[8]DeLancey, J. O. L. Anatomic aspects of vaginal eversion after hysterectomy. *Am. J. Obstet. Gynecol.* 166(6):1717–1728, 1992.

[9]Diwadkar, G. B., M. D. Barber, B. Feiner, C. Maher, and J. E. Jelovsek. Complication and reoperation rates after apical vaginal prolapse surgical repair: a systematic review. *Obstet. Gynecol.* 113(2):367–373, 2009.

[10]Donaldson, K., A. Huntington, and R. De Vita. Mechanics of uterosacral ligaments: current knowledge, existing gaps, and future directions. *Ann. Biomed. Eng.* 49(8):1788–1804, 2021.

[11]Donaldson, K., J. Thomas, Y. Zhu, S. Clark-Deener, M. Alperin, and R. De Vita. In-plane and out-of-plane deformations of gilt utero-sacral ligaments. *J. Mech. Behav. Biomed. Mater.* 131:105249, 2022.

[12]Giugale, L. E., A. I. Melnyk, K. M. Ruppert, G. S. Napoe, E. S. Lavelle, and M. S. Bradley. Total vaginal hysterectomy with uterosacral ligament suspension compared with supracervical hysterectomy with sacrocervicopexy for uterovaginal prolapse. *Obstet. Gynecol.* 138(3):435–442, 2021.

[13]Holt, E. US FDA rules manufacturers to stop selling mesh devices. *Lancet.* 393(10182):1686, 2019.

[14]Iwanaga, R., D. J. Orlicky, J. Arnett, M. K. Guess, K. J. Hurt, and K. A. Connell. Comparative histology of mouse, rat, and human pelvic ligaments. *Int. Urogynecol. J.* 27(11):1697–1704, 2016.

[15]Knight, K. M., P. A. Moalli, and S. D. Abramowitch. Preventing mesh pore collapse by designing mesh pores with auxetic geometries: a comprehensive evaluation via computational modeling. *J. Biomech. Eng.* 140(5):051005, 2018.

[16]Liang, R., S. Abramowitch, K. Knight, S. Palcsey, A. Nolfi, A. Feola, S. Stein, and P. A. Moalli. Vaginal degeneration following implantation of synthetic mesh with increased stiffness. *BJOG.* 120(2):233–243, 2013.

[17]Lowder, J. L., K. M. Debes, D. K. Moon, N. Howden, S. D. Abramowitch, and P. A. Moalli. Biomechanical adaptations of the rat vagina and supportive tissues in pregnancy to accommodate delivery. *Obstet. Gynecol.* 109(1):136–143, 2007.

[18]Luo, J., T. M. Smith, J. A. Ashton-Miller, and J. O. L. DeLancey. In vivo properties of uterine suspensory tissue in pelvic organ prolapse. *J. Biomech. Eng.* 136(2):021016, 2014.

[19]Luyckx, T., M. Verstraete, K. De Roo, W. De Waele, J. Bellemans, and J. Victor. Digital image correlation as a tool for three-dimensional strain analysis in human tendon tissue. *J. Exp. Orthop.* 1(1):1–9, 2014.

[20]Mallett, K. F., and E. M. Arruda. Digital image correlation-aided mechanical characterization of the anteromedial and posterolateral bundles of the anterior cruciate ligament. *Acta Biomater.* 56:44–57, 2017.

[21]Martins, P., A. L. Silva-Filho, A. M. R. M. Fonseca, A. Santos, L. Santos, T. Mascarenhas, R. M. N. Jorge, and A. M. Ferreira. Strength of round and uterosacral ligaments: a biomechanical study. *Arch. Gynecol. Obstetr.* 287(2):313–318, 2013.

[22]Miller, B. J., B. K. Jones, J. S. Turner, S. R. Caliari, and M. H. Vaughan. Development of a uterosacral ligament suspension rat model. *J. Vis. Exp.* 2022. https://doi.org/10.3791/64311.

[23]Moalli, P. A., N. S. Howden, J. L. Lowder, J. Navarro, K. M. Debes, S. D. Abramowitch, and S. L. Y. Woo. A rat model to study the structural properties of the vagina and its supportive tissues. *Am. J. Obstet. Gynecol.* 192(1):80–88, 2005.

[24]Nagelli, C. V., A. Hooke, N. Quirk, C. L. De Padilla, T. E. Hewett, M. van Griensven, M. Coenen, L. Berglund, C. H. Evans, and S. A. Müller. Mechanical and strain behaviour of human Achilles tendon during in vitro testing to failure. *Eur. Cells Mater.* 43:153–161, 2022.

[25]Nager, C. W., A. G. Visco, H. E. Richter, C. R. Rardin, Y. Komesu, H. S. Harvie, H. M. Zyczynski, M. F. R. Paraiso, D. Mazloomdoost, A. Sridhar, et al. Effect of sacrospinous hysteropexy with graft vs vaginal hysterectomy with uterosacral ligament suspension on treatment failure in women with uterovaginal prolapse: 5-year results of a randomized clinical trial. *Am. J. Obstet. Gynecol.* 225(2):153, 2021.

[26]Pack, E., J. Stewart, M. Rhoads, J. Knight, S. Clark, D. G. Schmale III., and R. De Vita. Effects of short-term moderate ZEN consumption on uterosacral ligament elasticity in pubertal gilts. *Res. Vet. Sci.* 133:202–209, 2020.

[27]Reay Jones, N. H. J., J. C. Healy, L. J. King, S. Saini, S. Shousha, and T. G. Allen-Mersh. Pelvic connective tissue resilience decreases with vaginal delivery, menopause and uterine prolapse. *Br. J. Surg.* 90(4):466–472, 2003.

[28]Rivaux, G., C. Rubod, B. Dedet, M. Brieu, B. Gabriel, and M. Cosson. Comparative analysis of pelvic ligaments: A biomechanics study. *Int. Urogynecol. J.* 24(1):135–139, 2013.

[29]Shahryarinejad, A., T. R. Gardner, J. M. Cline, W. N. Levine, H. A. Bunting, M. D. Brodman, C. J. Ascher-Walsh, R. J. Scotti, and M. D. Vardy. Effect of hormone replacement and selective estrogen receptor modulators (SERMs) on the biomechanics and biochemistry of pelvic support ligaments in the cynomolgus monkey (Macaca fascicularis). *Am. J. Obstet. Gynecol.* 202(5):485-e1, 2010.

[30]Smith, T. M., J. Luo, Y. Hsu, J. Ashton-Miller, and J. O. L. DeLancey. A novel technique to measure in vivo uterine suspensory ligament stiffness. *Am. J. Obstet. Gynecol.* 209(5):484-e1, 2013.

[31]Tan, T., F. M. Davis, D. D. Gruber, J. C. Massengill, J. L. Robertson, and R. De Vita. Histo-mechanical properties of the swine cardinal and uterosacral ligaments. *J. Mech. Behav. Biomed. Mater*. 42:129–137, 2015.

[32]Vardy, M. D., T. R. Gardner, F. Cosman, R. J. Scotti, M. S. Mikhail, A. O. Preiss-Bloom, J. K. Williams, J. M. Cline, and R. Lindsay. The effects of hormone replacement on the biomechanical properties of the uterosacral and round ligaments in the monkey model. *Am. J. Obstet. Gynecol.* 192(5):1741–1751, 2005.

[33]Vu, D., B. T. Haylen, K. Tse, and A. Farnsworth. Surgical anatomy of the uterosacral ligament. *Int. Urogynecol. J.* 21(9):1123–1128, 2010.

[34]Zernicke, R. F., D. L. Butler, E. S. Grood, and M. S. Hefzy. Strain topography of human tendon and fascia. *J. Biomech. Eng*. 106(2):177–180, 1984.